LAWRENCE
LIVERMORE
NATIONAL
LABORATORY

LLNL-JRNL-439176

Compression set in Gas Blown Condensation Cured Polysiloxane Elastomers

M. Patel, S. C. Chinn, R. S. Maxwell, T. S. Wilson, S. A. Birdsell

June 29, 2010

Polymer Degradation and Stability

Disclaimer

Elsevier Editorial System(tm) for Polymer Degradation and Stability
Manuscript Draft

Manuscript Number:

Title: Compression set in gas blown condensation cured polysiloxane elastomers

Article Type: Research Paper

Keywords: Foamed Polysiloxanes; Compression set; Stability; Ageing; NMR

Corresponding Author: Dr Mogon Patel,

Corresponding Author's Institution:

First Author: Mogon Patel

Order of Authors: Mogon Patel; Sarah Chinn; Robert S Maxwell; Thomas S Wilson

Abstract: Accelerated thermal ageing studies on foamed condensation cured polysiloxane materials have been performed in support of life assessment and material replacement programmes. Two different types of filled hydrogen-blown and condensation cured polysiloxane foams were tested; commercial (RTV S5370), and an in-house formulated polysiloxane elastomer (Silfoam). Compression set properties were investigated using Thermomechanical (TMA) studies and compared against two separate longer term ageing trials carried out in air and in dry inert gas atmospheres using compression jigs. Isotherms measured from these studies were assessed using Time-Temperature (T/t) Superposition. Acceleration factors were determined and fit to Arrhenius Kinetics. For both materials, the thermomechanical results were found to closely follow the longer term accelerated ageing trials. Comparison of the accelerated ageing data in dry nitrogen atmospheres against field trial results showed the accelerated ageing trends over predict, however the comparison is difficult as the field data suffers from significant component to component variability. Of the long term ageing trials reported here, those carried out in air deviate more significantly from field trials data compared to those carried out in dry Nitrogen atmospheres. For field return samples, there is evidence for residual postcuring reactions influencing mechanical performance, which would accelerate compression set. Multiple Quantum-NMR studies suggest that compression set is not associated with significant changes in net crosslink density, but that some degree of network rearrangement has occurred due to viscoelastic relaxation as well as bond breaking and forming processes, with possible post-curing reactions at early times.

Suggested Reviewers:

Compression set in gas blown condensation cured polysiloxane elastomers

Mogon Patel[1], Sarah Chinn[2], Robert S Maxwell[2],
Thomas S. Wilson[2], Stephen A Birdsell[3]

(1) Atomic Weapons Establishment (AWE), Aldermaston, Reading, RG7 4PR, UK
(2) Lawrence Livermore National Laboratory, Livermore, CA
(3) Los Alamos National Laboratory, Los Alamos, NM

Abstract

Accelerated thermal ageing studies on foamed condensation cured polysiloxane materials have been performed in support of life assessment and material replacement programmes. Two different types of filled hydrogen-blown and condensation cured polysiloxane foams were tested; commercial (RTV S5370), and an in-house formulated polysiloxane elastomer (Silfoam). Compression set properties were investigated using Thermomechanical (TMA) studies and compared against two separate longer term ageing trials carried out in air and in dry inert gas atmospheres using compression jigs. Isotherms measured from these studies were assessed using Time-Temperature (T/t) Superposition. Acceleration factors were determined and fit to Arrhenius Kinetics. For both materials, the thermomechanical results were found to closely follow the longer term accelerated ageing trials. Comparison of the accelerated ageing data in dry nitrogen atmospheres against field trial results showed the accelerated ageing trends over predict, however the comparison is difficult as the field data suffers from significant component to component variability. Of the long term ageing trials reported here, those carried out in air deviate more significantly from field trials data compared to those carried out in dry Nitrogen atmospheres. For field return samples, there is evidence for residual postcuring reactions influencing mechanical performance, which would accelerate compression set. Multiple Quantum-NMR studies suggest that compression set is not associated with significant changes in net crosslink density, but that some degree of

network rearrangement has occurred due to viscoelastic relaxation as well as bond breaking and forming processes, with possible post-curing reactions at early times.

Keywords: Foamed Polysiloxanes; Compression set; Stability; Ageing; NMR

List of Figures

1. **Introduction**

Flexible foamed polysiloxane rubbers play an important role in many specific applications including medical, electrical, and defence or military uses. Such materials require good long-term load retention capability as they often experience significant preload and exposure to complex aging environments while in service. The further development of new or improved material formulations thus requires predictive qualification studies to assess long-term (typically decades) reliability in function and safety. In order to do this, it is generally necessary to carryout accelerated ageing trials with a full appreciation that ageing behaviours can be complex, with ageing models developed over the short term not necessarily valid over longer timescales.

The mechanical recovery properties of a material are defined by the extent to which it regains its original dimensions after release from deformation, under the same environmental conditions as applied during the deformation stage [1]. Sufficient continual, short-term elastic recovery over service lifetimes of decades is necessary in order to prevent the formation of gaps and potential changes in dynamics of the subsystem or system. These preload decay rates are influenced by a combination of temperature dependant physical and chemical processes. Examples of the former are disentanglement processes caused by Rouse like dynamics, mobility of dangling chains, impurities, and plasticizers, and the formation or elimination of transient elastically inactive chains. Examples of the latter include chain scission and crosslinking reactions, slippage at filler surfaces, condensation at filler surfaces. Tobolsky, for example, originally postulated that the formation of new network linkages while under strain leads to permanent set [2]. These early predictions have been supported by multiple experimental and computational studies [3-12]. However, many of the common

ageing processes work against each other (i.e. crosslinking and chain scission) and may leave the average overall crosslink density unchanged yet may have significant effect on the overall network structure, and thus the static (set, modulus) and dynamic (modulus, creep, relaxation, etc) material properties. Unfortunately, few experimental methods provide sufficient insight in a sufficiently timely fashion to resolve the often competing contributions of these mechanisms to the recovery properties of polymeric composites.

Information in the open literature on the long term stability and ageing properties of gas blown cellular polysiloxane elastomers is very limited. From the information that is available, however, the most relevant study was that reported by Coons et al [18]. This assumed that the compression set (S) in cellular polysiloxane elastomers (in this case having an initial thickness of 1.14mm) follows a first order kinetic model shown below:

Equation 1 $$S = 1 - \exp(-k_T t)$$

Where k_T is the rate constant at temperature T and t is the age in years. An estimate of the rate constant at each temperature was obtained from the slope of a Ln (1-S) versus t plot. The temperature dependency was assumed to be consistent with the Arrhenius expression shown below:

Equation 2 $$K_T = \beta_1 \exp(-\beta_2 / RT)$$

where β_1 is the pre-exponential constant, β_2 is the activation energy, and R is the ideal gas constant (1.987×10^{-3} kcal/mol K). β_1 was estimated to be 1947 yr^{-1} and $\beta 2$ activation energy approximately 7.2 kcal/mol.

This study was a useful initial investigation into developing an understanding of compression set rates in thermally aged silicones, it did not however, clearly demonstrate the validity for first order kinetics, and this could be a source of uncertainty in predicted behaviour in the Coons model.

In this paper we report the results of our studies on foamed polysiloxanes materials thermomechanical measurements (TMA), long-term compression testing, real-time ageing data, and novel Multiple Quantum NMR. The successful use of many of these techniques for measuring mechanical property data relevant to the performance of foamed elastomers was first reported by the authors in an earlier publication [15]. Our studies to understand the ageing behaviour of foamed condensation cured siloxane materials is based on the use of these complex materials in many advanced specific load bearing applications in the defence industry. To date, and as a result of the technical challenges in monitoring long term behaviour in non-standard ageing environments, the open literature provides little guidance in understanding of the rate of change of key engineering properties influencing performance in these complex material systems. Such insight will provide key scientific basis for material selection for a number of technological applications in future systems. Thus the key objectives of this study were two fold: A) to validate the short term TMA method in its ability to deliver data relevant to long term life assessment, and B) obtain quantitative insight into the degradation rate/mechanisms including network structural changes occurring in these materials, and compare against data obtained from tests on samples from field trial.

2. Experimental

2.1 Materials

A number of different condensation routes are available for preparing a robust engineering silicone foam material including metal catalyzed condensation reactions that can produce endlinked networks of monomodal, bimodal, or multimodal chains [16,17]. Other mechanisms of network formation include the use of vinyl specific peroxide curing catalysts to produce endlinked, block, or random networks [17]. Formation of porosity can be achieved by a number of routes, including in-situ generation of gas bubbles through reaction (blown foams), and generation of porosity by network formation in the presence of sacrificial pore formers (usually prilled urea). In this paper our studies on condensation cured and hydrogen gas blown foams is reported. Figure 1 shows an example of the microstructure of such materials including evidence of damage to the cellular structure due to compression over extended time scales.

S5370 Material:

Foam elastomers were prepared from commercial kits (Dow Corning RTV5370), containing a base resin and catalyst resin. Foam elastomers were prepared by mixing 6 parts by weight of the catalyst resin to 100 parts of the base resin. As reported elsewhere [13, 15-16, 18, 42-44, 45-49], the composition of the mixed S5370 resin is thought to contain (by weight) approximately 15 % diatomaceous earth, 60% high molecular weight (Mw) polydimethylsiloxane (PDMS) diol, 12 % low Mw PDMS diol, 6 % polymethylhydrogensilane (PMHS), 5% diphenylmethylsilanol (DPMS), and 2% tetrapropylorthosilicate (TPS). The catalyst is predominantly stannous-2-ethylhexanoate. Crosslinking during foaming occurs due to tetra-n-propoxysilane and polymethylhydrogensilane. Crosslinking reactions together with in-situ generated hydrogen

gas bubbles leads to a foamed polymer that is compression moulded and postcured at 120 ^{o}C for 24 hr. This long-term bake out procedure at elevated temperature was used to minimise any residual postcuring effects. At the same time recent publications have identified multiple post-curing reactions [42 to 44]. The bulk density of the foams produced using this method were typically 0.5 g cm^{-3} and 0.8 g cm^{-3} (prepared through controlled pre-compression of the material curing moulding and curing operations).

Silfoam Material:

As the polysiloxane ingredients used in S5370 formulations are now no longer commercially available, in-house development activities have identified Silfoam as a potential replacement material. The manufacturing process for this material is similar to that detailed for S5370. Silfoam is produced from condensation reactions of PDMS chains with two average molecular weights obtained from Gelest (18 wt. % Low molecular weight dimethyl siloxane gum and 60 wt. % high molecular weight dimethyl siloxane resin), a Diphenylmethylsilanol chain end capper (5 wt %,) and using the multifunctional crosslinking site (Polymethyhydrosiloxane 5 wt%; Gelest). Curing is catalyzed with tetraalkoxysilicate curing agent (2 wt%) and the material is filled prior to curing with the high surface area silica filler HiSil 233 silica (a reinforcing filler; 10 wt %).

2.2 Thermomechanical Ageing Experiments

Details of the thermomechanical analyser (TA Instruments TMA 2940) used in these studies have been reported in an earlier publication [16] and therefore will not be discussed in detail.

Briefly, the instrument was used in intermittent stress relaxation mode by applying a fixed compressive strain (25% strain) to the elastomer held at a controlled temperature. The applied load/strain was removed and reapplied at controlled intervals, with the material allowed to recover for typically 30 minutes after which there was no further significant recovery.

The percentage compression set was determined by taking the ratio of the loss in sample thickness (original thickness minus the thickness after recovery) over the original thickness (the denominator). Our thermomechanical studies were carried out over time and using a range of temperatures from ambient (21 ^{o}C) to 130 ^{o}C. These experiments were performed in a dry nitrogen gas atmosphere with thermal expansion effects of the probe and the stage accounted for by measuring the baseline at any given temperature.

2.3 Long-term ageing studies

Ageing studies carried out at Lawrence Livermore National Laboratory (LLNL) involved the use of custom made compression jigs like the one shown in Figure 2. These jigs were loaded with S5370 pads (typically >0.7 g cm^{-3} bulk density) and placed into a environmental chamber with a dry nitrogen gas flow atmosphere. At one month intervals, the compression jig was removed and allowed to equilibrate with room temperature. The compression jig was then attached to a MTS model 632.11B-20 instrument and after removal of the compression bolt, the cross head was raised (load was removed) at 0.0008 inch per minute for 0.040 inch of travel, or well after any load remains on the specimen. At this point the crosshead was lowered at 0.0008 inch per minute until a minimum load of 275 lbs force was applied to the test fixture gauge blocks. At this point the crosshead was reversed at the same speed and the procedure repeated for a total of three load-unload cycles to breakdown potential hysteresis effects. The force and displacement were recorded as a function of time for each cycle. The

thickness was estimated using the displacement at which the load was first observed to increase. The estimated measurement error associated with making this measurement was +/- 10 microns.

For comparison purposes, additional S5370 aging data considered here was obtained from studies carried out by Los Alamos National Laboratory (LANL) and Kansas City Plant (KCP). These studies have previously been reported by Coons et al [18] and for this reason have not been discussed in detail here. Briefly, these studies involved the compression of S5370 samples (typically 0.5 g cm^{-3} bulk density) to 50% of their original thickness (1.14mm) in stainless steel jigs. Thickness and compressive property measurements were made prior to loading the samples into the fixtures, and periodically throughout the ageing study. The duration of these experiments was 9 years in air at a number of different temperatures from 23^{o}C to 70^{o}C.

2.4 Theoretical Treatment

Acceleration factors (a_T) derived from Time-Temperature (T/t) superposition has been commonly used to assess the extent of temperature sensitivity in polymer elastomers [13]. The underlying process may have significant contributions from changes in free-volume as described by the Williams-Landel-Ferry model (WLF). This assumes that the free volume is a linearly increasing function of temperature above the glass transition temperature [19]. C1 and C2 are WLF constants (typically 17.44 and 51.6 respectively). C1 correlates to the inverse of free volume in the amorphous system at the T_g, while C2 is correlated to the ratio of free volume at T_g to the increase in free volume with thermal expansion above T_g. The WLF universal constants were originally derived from data from various types of synthetic

polymers but are system-dependent and are not expected to be valid for all materials. The WLF kinetics typically holds at temperatures between T_g and T_g + 100 (°C) for amorphous systems and siloxane materials having typically very low T_g's are not known to obey this model [19, 20].

Alternatively, the temperature variance may be described by the Arrhenius equation, which, of course, relates the apparent activation energy required for a dynamic process such as polymer segment movement to unoccupied areas (holes), the rearrangement of chains towards new configurations in equilibrium at the new perturbed (strained) state, the formation of new crosslinks or fracture of chains [21]. Arrhenius kinetics predicts that either increasing the temperature or decreasing the activation energy (e.g. through catalysts) will increase the rate of reaction and can be used to validate whether the rate doubling effect of temperature holds.

2.5 Multiple Quantum NMR

As a supporting technique to help assess mechanistic information both static and multiple quantum NMR experiments have been performed on virgin and aged S 5370 materials. Static NMR experiments were performed on a Bruker Avance 400 spectrometer with a ^1H frequency of 400.13 MHz. Samples with dimensions sufficiently small to fit within the diameter of a typical 5 mm sample tube (~ 3 mm x 3 mm x 2 mm) were centered within the coil volume of a Bruker TBI (HCX) 5 mm probe with 90º pulse lengths τ_p = 4.50 to 5.25 μs. Multiple Quantum NMR experiments were performed as described elsewhere [22-27] using the generic pulse sequence described in those references to excite even-quantum coherences.

The MQ-NMR growth curves were analyzed using fast Tikhonov regularization software using the Kernal function:

Equation 3 $$y = 0.5 \times \left(1 - \exp\left(-\left(0.378 * 2\pi\langle\Omega_d\rangle\right)^{1.5} \tau^{1.5}\right)\cos\left(0.583 * 2\pi\langle\Omega_d\rangle\tau\right)\right)$$

Where the kernal function incorporates a slight maximum that is often observed in the normalized data [28]. In this version of the regularization routine, the program automatically varies an error parameter and corresponding χ^2 parameter, or the mean squared deviation between the data and the fit. The distribution with the minimum χ^2 below which the χ^2 value remained relatively constant was picked for the analysis. The output of this analysis is a distribution of residual dipolar couplings [22-27]. It has been shown that the dynamic order parameter and the residual dipolar coupling can be related to the number of statistical segments between physical or chemical constraints:

Equation 4 $$S_b = \frac{1}{P_2(\cos\alpha)} \frac{\langle\Omega_d\rangle}{\langle\Omega_d\rangle_{static}} = \frac{3r^2}{5N}$$

where the static dipolar coupling, $\langle\Omega_d\rangle_{static}$, is averaged by the rotation of the methyl groups in PDMS, $P_2(\cos\alpha)$ is the second order Legendre polynomial describing the orientational changes between the dipolar vector and the chain axis, and *r* describes the distance relationship between the end-to-end vector, R, from that of the unperturbed melt.

In swollen networks, a number of theories have been developed to understand the response of the network to solvent induced strain [29, 30]. For the purposes of the work described here, it is evident that upon swelling in Toluene (a good solvent for PDMS) the MQ growth

curves are perturbed due to the modification of the chain segmental dynamics by the introduction of the solvent. It has been shown that for a number of silicone networks the response of the MQ-NMR derived distributions of residual dipolar couplings can reveal otherwise hidden aspects of the network structure [22, 31]. For these swelling experiments, the small sample used for NMR analysis was submerged in d_5-toluene for 3-7 days in order to reach equilibrium swelling. The MQ-NMR experiment was then performed and the data analyzed after removing any spectral contributions due to the residual ^1H content of the toluene solvent. The MQ growth curves were then analyzed in the same fashion as the data obtained on non-swollen networks.

3. Results and Discussion

3.1 Thermomechanical Studies

The results from TMA studies for S5370 are shown in Figure 3A. Each isotherm shows an increase in % compression set with time, with an increase in the rate of compression set with increasing temperature. The isotherms were then superimposed on the lowest temperature data set by horizontally shifting each isotherm along the time axis using a constant scaling factor for each temperature (better known as the Acceleration Factors). This treatment uses all the available data points to obtain a master curve showing a best fit of superimposed data, see Figure 3 B. This reveals increased data scatter over short periods and is indicative of the very small changes in sample thickness. Over longer times however, the data exhibits reasonable good linear behaviour.

Figure 4 shows a comparison of S5370 against the Silfoam material. This shows that the rate of change in sample thickness with age for S5370 is not too dissimilar to that of Silfoam,

which isn't surprising given the similarities in network structure – though the amount and type of fillers differ. S5370 has typically ~ 15 wt% diatomaceous earth whereas Silfoam has HiSil 233 silica to 10 wt % loading. This difference in filler constituent does not appear to significantly alter the ageing characteristics. The difference in filler type and content does not seem to have a significant effect on the compression set kinetics. This is somewhat surprising and though the two networks are similar, they are not equal and the offsetting effects of differences in network structure and filler content may mask contributions to one or the other.]

3.2 Long term accelerated ageing trials

Isotherms for S5370 obtained from the LLNL long term compression ageing study are summarised in Figure 5A. Using T/t analysis, a master curve was obtained at the lowest test temperature and is shown in Figure 5B. There is significant scatter in the experimental data at early times that complicated the time shifting necessary for the T/t analysis. The testing methodology for this study was subject to significantly larger sources of error than the thermomechanical approach, particularly for the small changes in thickness observed at room temperature and over short times. A linear regression fit of ln(S) as a function of time allows the sample thickness (T_t) to be expressed by equation 1 where t is the age in years and T_o is the initial sample thickness (mm). A polynomial fit allows the % compression set (S) to be expressed as:

Equation 5: $$S(\%) = -6x10^{-5}\ t^3 - 0.0025\ t^2 + 0.4331\ t\ + 1.0465 = \left(\frac{T_o - T_t}{T_o}\right) X\ 100$$

Where T_o is the initial thickness (mm), t (yr) is the age and T_t is the recovered thickness.

Similarly, the results of the accelerated ageing studies carried out by KCP-LANL and reported by Coons et al [32] are shown in Figure 6. Each data set showed increasing % compression set with time, and an increase in the rate of compression set with increasing temperature. The raw data from this study has been obtained and subjected to T/t. analysis, and Figure 7 shows the master plot generated from the analysis. Although there is again some scatter in results at early times due to the same experimental limitations mentioned above, the superimposed data shows a reasonably good linear trend. A linear regression fit allows the % compression set (S) to be expressed as:

Equation 6 $$S(\%) = 0.56\ t = \left(\frac{T_o - T_t}{T_o} \right) X\ 100$$

A comparison of the TMA ageing results against both the LLNL and KCP-LANL long term accelerated ageing data for S5370 is shown in Figure 8. The TMA data represented by the data trend at early times follows closely the same trend as the long term ageing data trends. The agreement in behaviour measured by two different techniques helps validate the TMA results and provides confidence that the ageing trend is most probably a true reflection of the behaviour of the material. However some caution is required as short term ageing experiments on foamed S5370 materials can predict ageing trends that can be significantly different to those predicted from longer term trials [18]. A possible reason for this is potential residual crosslinking reactions that can dominate the early time ageing properties and which may be minimised through effective baking out of materials at elevated temperatures prior to use in ageing trials. An additional complication may arise due to the presence of active catalyst (tin II) in the short term work whereas over the long term the catalyst can de-activate to tin IV as reported in the open literature [48].

The difference in trends between the KCP-LANL data and the LLNL long term compression studies reported here is largely due to the fact that the latter studies were performed in dry nitrogen atmospheres, whereas the KCP-LANL studies were carried out in air. An additional contributing factor to this variation is that LLNL studies were performed on high density material, whereas the KCP-LANL study was performed on low-density foam compressed to higher levels. Silicone based materials are well known to suffer hydrolysis degradation effects during service and these effects can be minimised by reducing the relative humidity by the use of dry nitrogen. For this reason, it is believed that the effects of air vs. nitrogen difference would far outweigh any potential ageing differences from foam density variation.

3.3 Temperature Dependency

To assess whether the observed differences in compression set with time and temperature were due to differences in underlying degradation mechanisms, an analysis of acceleration factors (derived from T/t treatment) for temperature sensitivity was made. Plots of acceleration factor obtained from both short and long term experiments as a function of inverse temperature are shown in Figure 9. The temperature dependency of the rate constants is consistent with a single activation energy mechanism.

There was no indication of significant changes in the slope of the plot (from which the activation energy can be derived) at temperatures up to 130^{o}C for the thermomechanical studies. For both S5370 and Silfoam, the apparent activation of the underlying degradation process is not too dissimilar, typically 37 ± 4 kJ/mol, although the LLNL study tended to predict a higher temperature dependency than the other trials (see Table 1). Furthermore, the activation energy values for S5370 from TMA studies are in close agreement to values

reported from the longer term ageing trials, and are consistent with numerous ageing mechanisms including acid catalysed hydrolysis and network rearrangement [18].

3.4 Comparison against field trials data

Field trials data from tests on service returns (real-time aged) have been included in this study as a comparison against predictions from the long term accelerated ageing results. Figure 10 shows field trials data expressed as recovered thickness as a function of service time. Field return S5370 components show a gradual loss in recovered thickness indicative of compression set. The large data scatter is indicative of the significant component-to-component variability in service components. On comparing the field return data with accelerated, it is evident that both the LLNL (Equation 5) and KCP-LANL (Equation 6) models tend to over predict the rate, with perhaps the LLNL model closer in line with the real-time data. The LLNL study, unlike the KCP-LANL work, was carried out in low humidity dry nitrogen atmospheres that more accurately mimic in-service conditions. For comparison purposes, Figure 10 also incorporates the prediction from the ageing model reported by Coons et al (see Equation 1).

Although comparison in each case is difficult as the field return data shows significant data scatter indicative of component to component variability, the Coons model tends to under predict the rate for all the field trials data and this could be due to the fact that the model assumes a first order kinetic rate equation that may possibly be too simple to describe the compression set properties in these complex materials.

These differences between accelerated and real-time behaviours provide a good example of the complexity of the material system the properties of which can be highly variable. It's worth noting that time-temperature (T/t) superposition as been used as the data analysis

routine of choice here because other analysis methods such as kinetic rate functions have not been successfully identified for this material. The large scatter observed here in many of the isotherm trends (see Figure 5 and Figure 7) makes the use of T/t problematic, potentially leading to inaccurate predictions.

3.5 Engineering Stress

One of the key engineering interests in the ageing properties of cellular polysiloxanes is the assessment of stress versus strain profiles and how these profiles change as a function of age. The stress required to compress the material to a given strain (denoted the engineering stress) typically decreases as a function of time [18]. Engineering stress measurements are typically made on the fourth test run after cyclic stress-strain experiments. Figure 11 shows the results from mechanical studies on service return S5370 samples. Although the results show significant data scatter indicative of component to component variability, in each case a clear age related trend cannot be assigned. A large proportion of the results are consistently above specification, especially at early times. This perhaps may be partly explained by residual postcuring reactions influencing predominately the early time response and which would accelerate compression set. Future work using finite element modelling codes will be used to assess how these age related changes might impact or influence system dynamics.

3.6 MQ NMR

Distributions of residual dipolar couplings (RDC) obtained from regularization of MQ NMR growth curves for S5370 samples unaged, aged at 25 ^{o}C for 2 yr and 70 ^{o}C for 2 yrs are shown in Figure 12. Bimodal distributions were observed for both polymer formulations. The bimodal distribution obtained for S5370 reflects the bimodal distribution of molecular

weights of the starting materials [22, 27]. The near-Gaussian shape of the distributions has been observed previously as well and it has been noted that this is in contrast to the distributions expected from a Gaussian distribution of chain end-to-end vectors [24, 25]. For the purposes of the study here, the exact shape of the distribution is not of primary concern, but rather the net changes in the distribution. Discussions of and direct comparisons of these distributions are discussed elsewhere [25, 33]. Overall, no significant differences in distributions were observed as a function of time or temperature. This would indicate that negligible chemical degradation has occurred and that the permanent set was predominately due to physical rearrangement of the network chains rather than the formation of new chemical crosslinks.

It is possible; however, that equal chain scission and chain reformation processes that does not dramatically alter the net crosslink density distribution exist. It has been shown that additional information on the network structure can be obtained by characterizing the changes in the residual dipolar coupling occurring as a result of swelling the network in a good solvent, as discussed in the experimental section [27, 31]. Distributions of RDCs of the same set of samples swollen in toluene are also shown in Figure 12. Upon swelling the distributions became broader with significant population both at higher and lower general average RDC. This behaviour is similar to that seen by Saalwächter et al and by Gjersing et al for similar networks and reflects the strong degree of swelling heterogeneity and the non-affine nature of the network chain deformations. In both the control and the 70 ^{o}C sample, upon swelling, the lower molecular weight chains (lower RDC) were found move from a maximum RDC of ~ 0.16 kHz to 0.08 kHz for the material aged at 70 ^{o}C and 0.11 kHz for the material aged at 25 ^{o}C. The chains with higher RDCs seem to be more strongly affected

by swelling in toluene than the longer network chains. The average RDC for these chains has been reduced from ~ 0.6 kHz to ~ 0.4 kHz (25 ^{o}C) or ~ 0.3 kHz (70 ^{o}C). The width of the distribution for the longer chains is also narrower for the material aged at 25 ^{o}C. This data is similar to data obtained on other silicone networks. In general, swelling acts inhomogeneously to relax the majority of chains (general decrease in maximum RDC), while stretching others (increased broadening of distribution). Of notable exception of the general agreement with Saalwächter, et al [24] (where the shorter chains were observed to have the RDC characterizing them increase, the shorter chains have been observed to decrease here. The network structure studied here is significantly different than the simple bimodal network reported in the open literature [31], constructed from higher molecular weight starting materials (MW_{long} ~ 58000 g/mol; MW_{short} ~ 1900 g/mol) and the use of the multifunctional crosslinking species poly(methylhydrogensilane). The network structure in S5370, thus allows for significantly more cooperative motion and the development of fewer highly strained chains.

The MQ-NMR data shown in Figure 12 is evidence that despite the overall segmental dynamics and average order parameter remaining unchanged at room temperature and in the unstrained state, the network structure has been altered in a fundamental way. The occurrence of thermally induced chain scission reactions (breaking of siloxane linkages), thermally induced condensation of silanol to siloxane linkages and postcuring reactions involving residual silane sites, while the network physically rearranges due to viscoelastic relaxation is consistent with this observation. Further, the occurrence of these reactions has been observed in other studies in similar materials [27, 34-44]. Since this data suggests that

new crosslinks have formed and that the network structure has changed, the observance of compression set in these materials is fully consistent with the Tobolsky model.

4. Conclusions

Condensation cured hydrogen blown materials have a number of specialised load bearing applications in ageing regimes that are usually complex and non-typical. As ageing data in the open literature is very limited on these materials, our studies have attempted to shed light on likely long term performance characteristics. Thermomechanical trials show that the ageing behaviour of S5370 is not too dissimilar to Silfoam, a material developed as a potential replacement. Both these materials show similar temperature dependencies and the results support Silfoam as a suitable replacement for S5370. The results from thermomechanical studies are validated by the long term ageing studies carried out using compression jigs.

Comparison of accelerated ageing trials carried out in air and in dry Nitrogen atmospheres against field trials data shows that the accelerated ageing results overestimate the age related trend. These differences may be due to the in-service components experiencing complex ageing regimes that may not be adequately reproduced in accelerated ageing trials. Our NMR studies suggest that compression set is not associated with significant changes in crosslink density, but more likely a reorganisation of the network. Overall, our studies provide valuable insights into the likely long term engineering performance of these complex technically challenging materials.

Acknowledgements

The authors would like to thank Los Alamos National Laboratory (NM) and Kansas City Plant (Honeywell FM&T, Kansas City, MO) for the 9 yr accelerated long term ageing data on S5370, as well as field trials data on S5370. Part of this work was performed under the auspices of the U.S. Department of Energy by Lawrence Livermore National Laboratory under Contract DE-AC52-07NA27344. The authors would also like to thank Mark Pearson, Al Shields, and Greg Larsen for help measuring the compression set in the long term ageing trials.

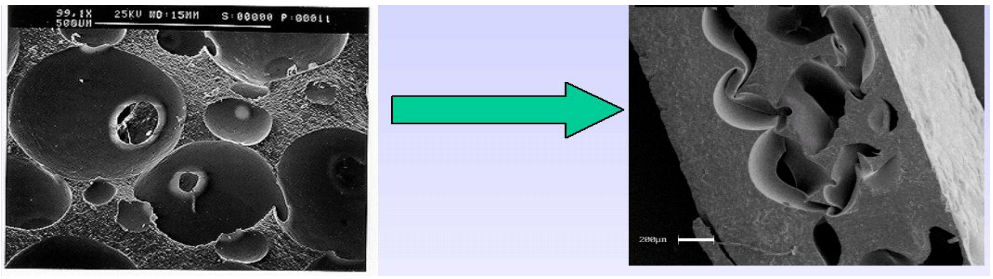

Figure 1: Gas blown condensation cured polysiloxanes are used in a number of load bearing applications within the defence industry. The Scanning Electron Microscope Image before and after service use shows evidence of significant damage to the microstructure.

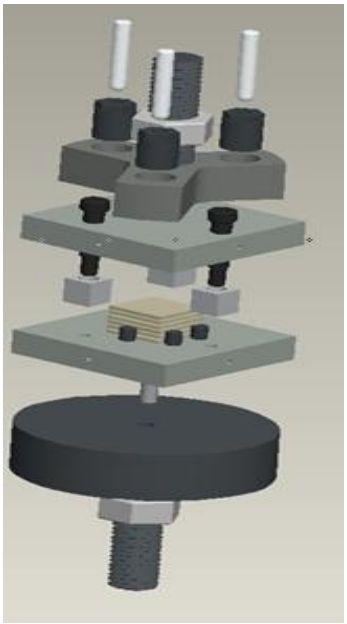

Figure 2: Long term compression ageing studies reported here utilised three 1.5” diameter S5370 pads which were stacked with spacers into a custom made compression jig

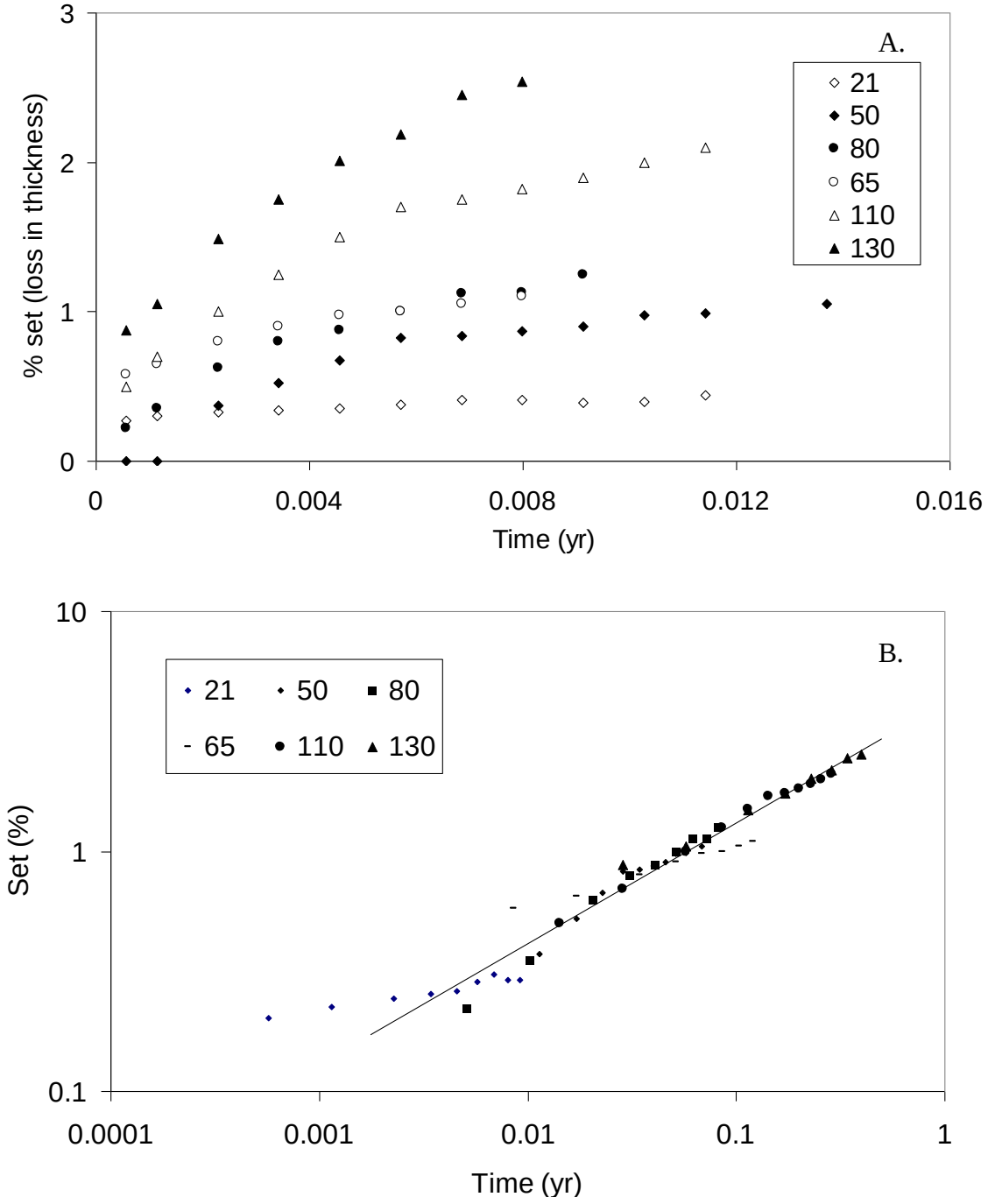

Figure 3: Data generated from thermomechanical trials carried out in dry nitrogen atmospheres at a number of different temperatures with 25% compressive strain on the

sample. **Top (A)**, isotherms generated from studies on S5370; **bottom (B)** double log master plot at 21^{o}C generated from T/t analysis.

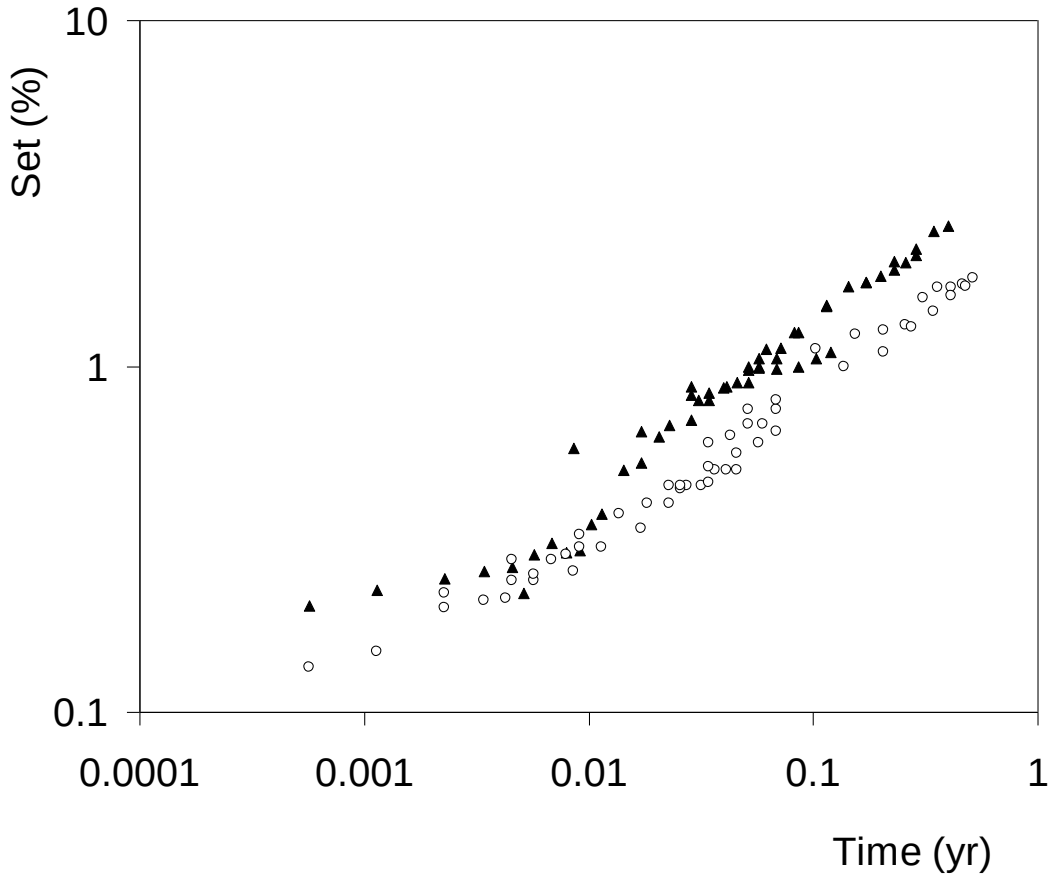

Figure 4: Thermomechanical ageing data from Silfoam (open circles) compared against S5370 (closed triangles). The in-house formulated elastomer (Silfoam) exhibits essentially similar ageing characteristics to S5370.

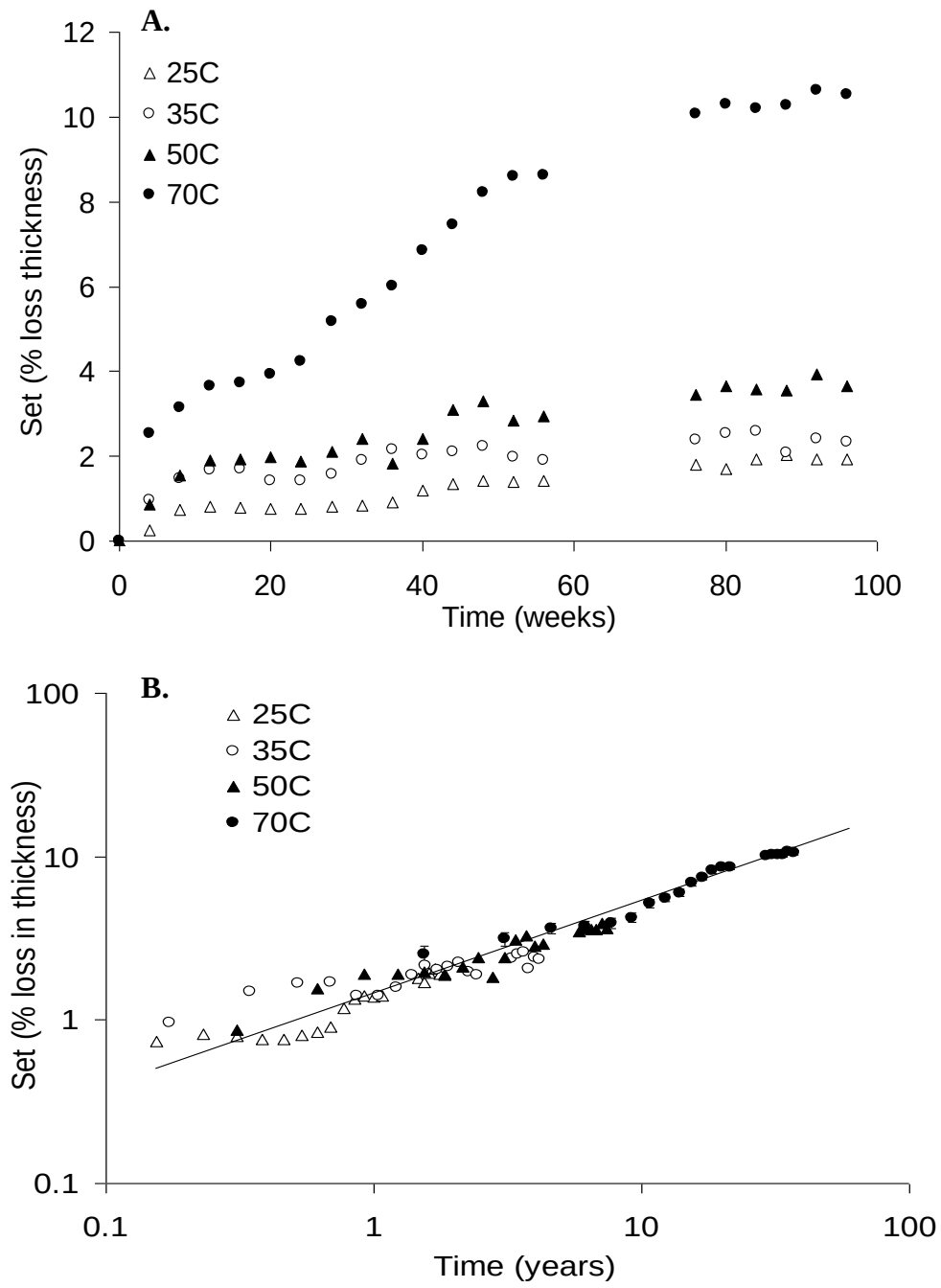

Figure 5: Ageing experiments carried out for this study in long term compression aging in dry nitrogen atmospheres at different temperatures with 25% compressive strain. **Top (A)**, isotherms generated from studies at a range of different temperatures; **Bottom (B),** double log master plot at 25^{o}C from T/t analysis at the lowest reference temperature.

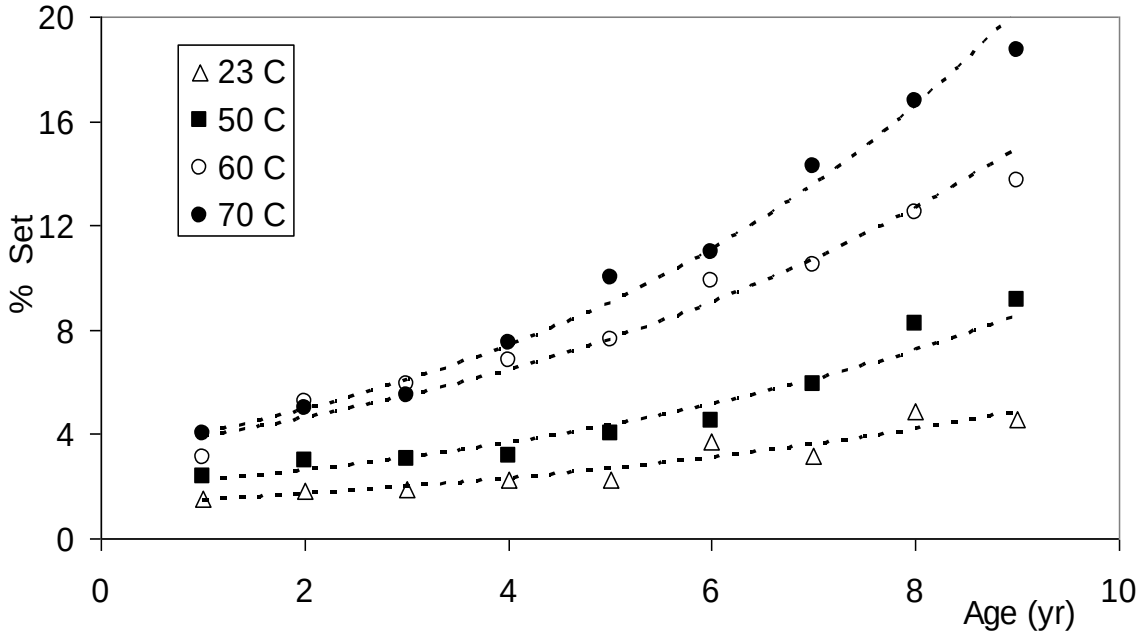

Figure 6: KCP-LANL accelerated ageing trials on S5370 in air at different temperatures with 50% compressive strain.

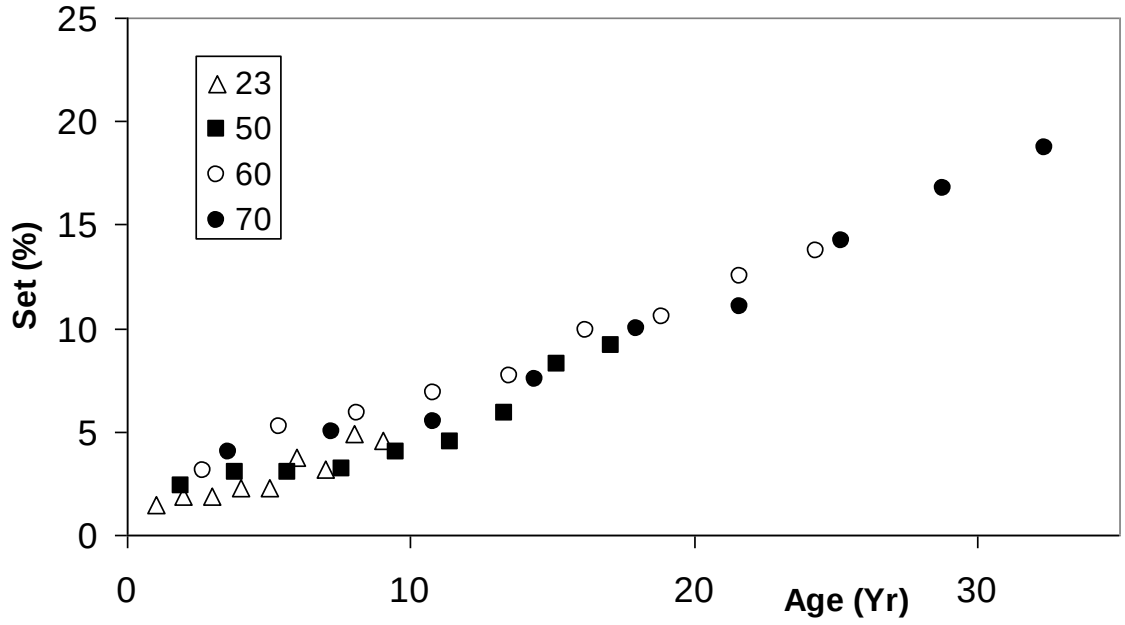

Figure 7: Master plot at 23°C from T/t analysis of the KCP-LANL accelerated ageing data

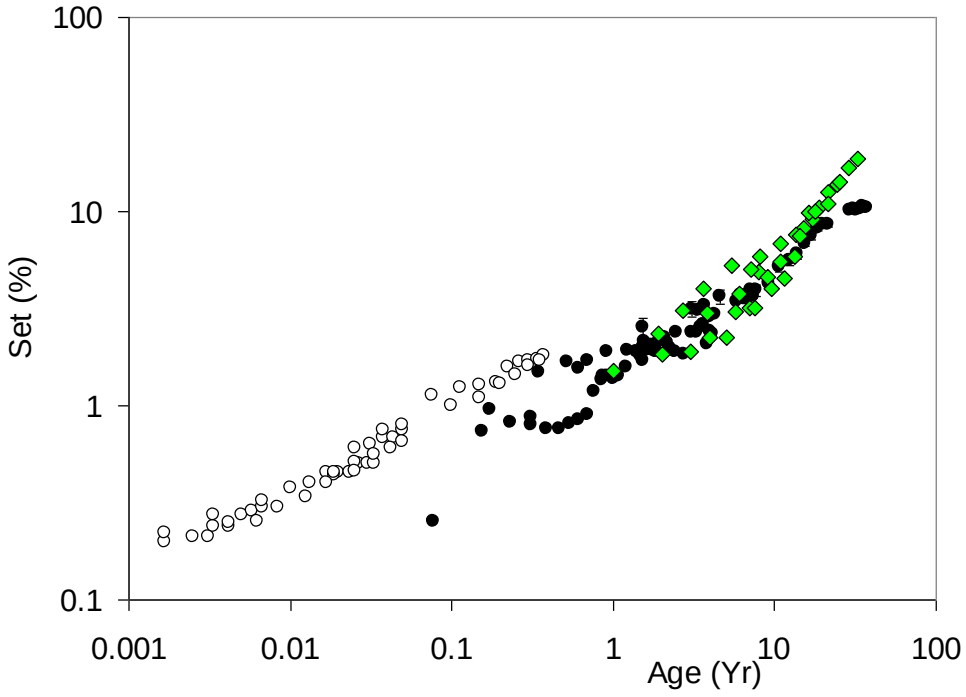

Figure 8 : Compression set as a function of age for S5370 from the various ageing trials: Thermomechanical accelerated ageing method (open circles); KCP-LANL accelerated ageing trials (diamond); and LLNL accelerated ageing data (solid black circles).

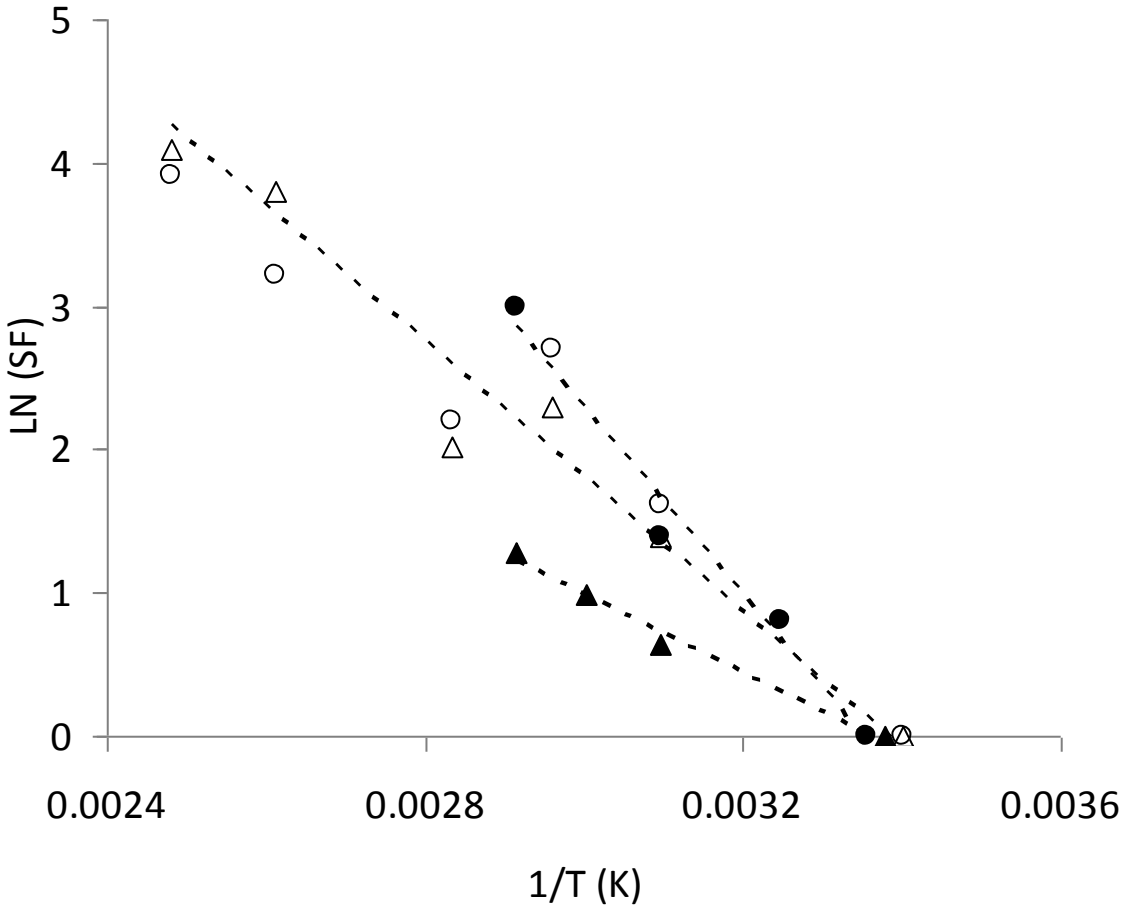

Figure 9: Arrhenius plot showing the temperature dependency of acceleration factors (SF) generated from T/t analysis: Thermomechanical accelerated ageing work (open circles); KCP-LANL accelerated ageing study (solid triangles); LLNL accelerated ageing study (solid circles); accelerated ageing studies on Silfoam using Thermomechanical (open triangles).

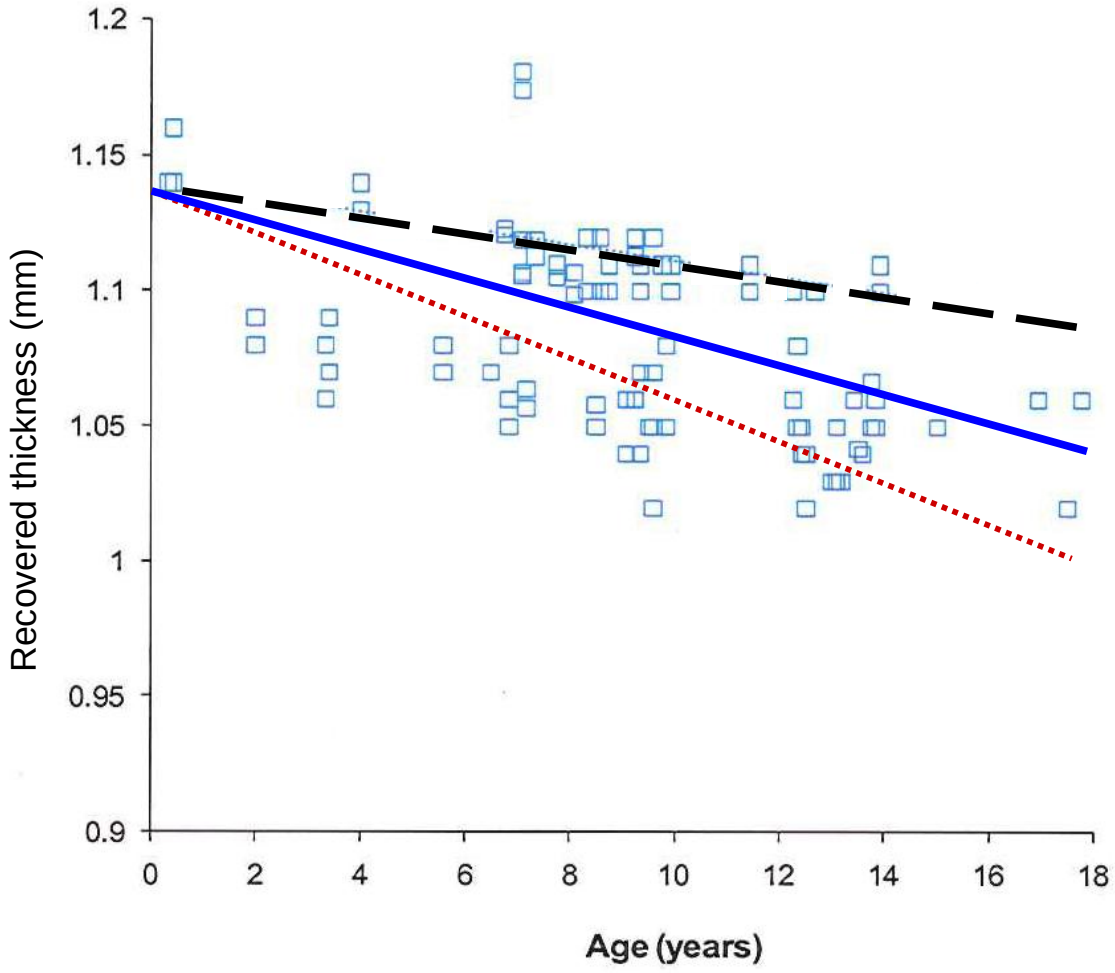

Figure 10 : Comparison of field trials data versus predictions from accelerated ageing. Thickness as a function of age for S5370 components; Black dash line (Coon's model, Equation 1), KCP-LANL model (Equation 6, red dash line); LLNL model (Equation 5, blue solid line).

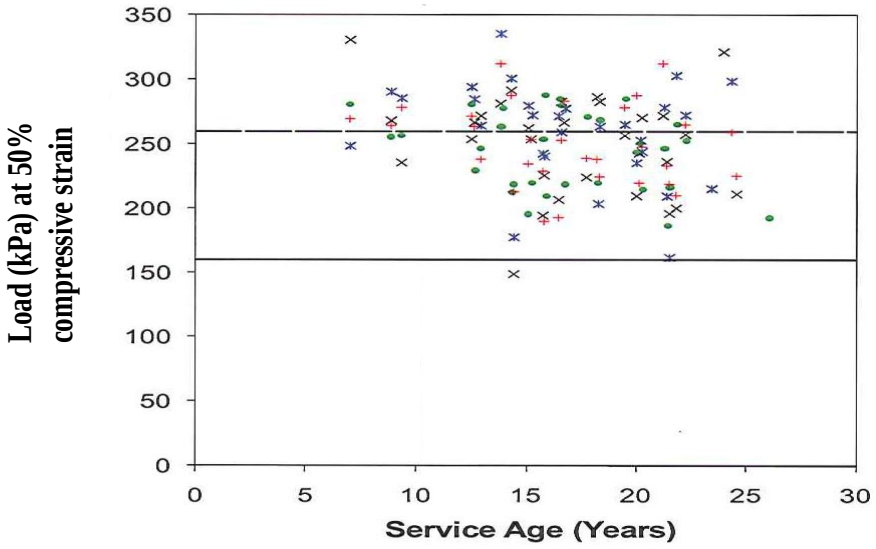

Figure 11: Load at 50% compression as a function of component service age.

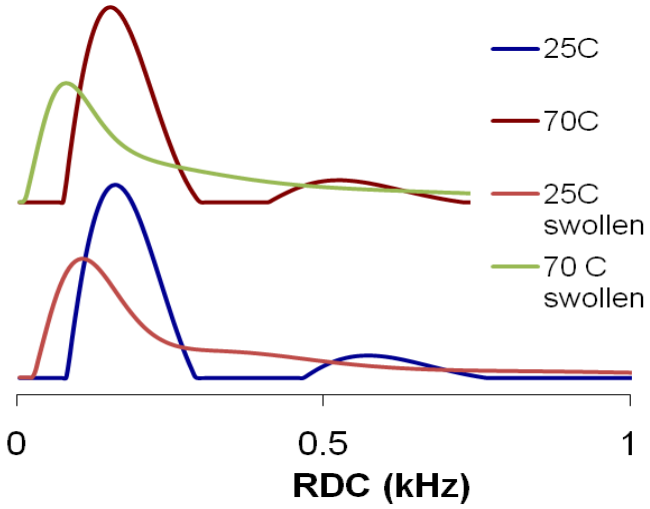

Figure 12: The results from MQ-NMR in the unswollen state and the swollen state (in toluene). Results show the distributions of residual dipolar couplings (RDC) for S5370 aged at 70 ^{o}C and 25^{o}C for 2 yr under compression

Material	Data Source/study	E_a (kJ/mol)
Silfoam	TMA	37 ± 4
S5370	TMA	33 ± 4
	LANL-KCP	23 ± 4
	LLNL	54 ± 10
S5370	Coons study [18]	30 ± 4

Table 1: A summery of Arrhenius activation energies.

References

1. Tolbolsky AV. "Properties and Structure of polymers" (1960) Wiley, New York, 306
2. Andrews RD, Tobolsky AV, Hanson EE; J Appl Phys 1946;17:352e61.
3. Rottach DR, Curro JG, Grest GS, Thompson AP; Macromolecules 2004;34:5468e73.
4. Maiti A, Gee R.H, Weisgraber T, Chinn S, Maxwell R.S.; Polym Deg Stab 93 (2008) 2226–2229
5. Todd H. Weisgraber, Richard H. Gee, Amitesh Maiti, David S. Clague, Sarah Chinn, Robert S. Maxwell; Polymer 50 (2009) 5613–561
6. Gillen, KT; Bernstein, R; Wilson, MH Predicting and confirming the lifetime of o-rings Polym Deg Stab, 87 (2): 257-270 Feb 2005
7. Baxandall, LG; Edwards, SF; Macromolecules, 21 (6): 1763-1772 Jun 1988
8. Gillen, KT;Macromolecules, 21 (2): 442-446 Feb 1988
9. Murakami, K; Tamura, S; Journal Of Polymer Science Part C-Polymer Letters, 10 (12): 941-943 1972
10. Evrard, G; Job, C; Journal Of Polymer Science Part A-2-Polymer Physics, 5 (6pa2): 1029-& 1967
11. Flory, PJ 'Elasticity Of Polymer Networks Cross-Linked In States Of Strain' *Transactions Of The Faraday Society*, 56 (5): 722-743 1960
12. Chinn, S; DeTeresa, S; Sawvel, A; Shields, A; Balazs, B; Maxwell, RS**;** Polym Deg Stab, 91**,** 555-564, (2006).
13. Patel M, Skinner AR. Polym Degrad and Stab 2001;73:399.
14. Wright D. "Failure of Plastics and Rubber Products" (2001) Rapra Technology, 178.
15. Patel M, Morrell PR, Murphy JJ; Poly Deg Stab. 2005; 87:201
16. Patel M, Soames M, Skinner AR, Stephens TS. Polym Degrad and Stab 2004:83:111

17. Brook MA. Silicon in organic, organometallic, and polymer chemistry. New York: Wiley; 2000.
18. Coons JE, McKay MD, Hamada MS; Polym Deg Stab. 91(2006) 1824-1836
19. Lomellini P. Polymer 1992:33:23:4983
20. Williams ML, Landel RF and Ferry JD (1955) J Amer Chem Soc 77, 3701-3707.
21. Ferry, J. D., "Viscoelastic properties of polymers", 2nd edition. (1970) Wiley, New York:
22. Gjersing, E.; Chinn, S.; Maxwell, R. S.; Giuliani, J. R.; Herberg, J.; Eastwood, E.; Bowen, D.; Stephens, T. Macromolecules 2007, *40*, 4953- 4962.
23. Saalwächter, K. *J. Am. Chem. Soc.* 2003, *125*, 14684-14685.
24. Saalwächter, K. *J. Chem. Phys.* 2004, *120*, 454-464.
25. Saalwächter, K. *Prog. NMR Spectrosc.* 2007, *51*, 1-35.
26. Maxwell, R. S.; Chinn, S. C.; Solyom, D.; Cohenour, R. Macromolecules 2005, *38*, 7026-7032.
27. Jason R. Giuliani, Erica L. Gjersing, Sarah C. Chinn, Ticora V. Jones, Thomas S. Wilson, Cynthia T. Alviso, Julie L. Herberg, Mark A. Pearson, and Robert S. Maxwell, *J. Phys. Chem. B* 2007, *111*, 12977-12984
28. Chinn, S.C., Alviso, C.T., Berman, E.S.F., Harvey, C.A., Maxwell, R.S., Wilson, T.S., Cohenour, R., Saalwächter, K., Chassé, W., MQ NMR and SPME analysis of nonlinearity in the degradation of a filled silicone elastomer. *J. Phys. Chem. B,* in press (2010)
29. Flory, P J, Rehner, J, Jr. J Chem Phys 1947 11 512
30. Sperling, LH Physical Polymer Science, John Wiley & Sons, Danvers, 2001
31. Saalwachter, K.; Kleinschmidt, F.; Sommer, J. U. *Macromolecules* 2004, *37*, 8556-8568.
32. Mayer, B, Reimer, J., Maxwell, R. S., Chinn, S., *Chem. Eng. Sci*, 64, 4684-4692 (2009).
33. Hall, A. D.; Patel, M. *Polym. Degrad. Stab.* 2006, *91*, 2532-2539.
34. Thomas, D. K. *Polymer* 1966, *7*, 99.
35. Zeldin, M.; Qian, B. R.; Choi, S. J. *J. Polym. Sci. Part A*sPolym. Chem. 1983, *21*, 1361-1369.
36. Grassie, N.; Macfarlane, I. G. *Eur. Polym. J.* 1978, *14*, 875-884.
37. Grassie, N.; Macfarlane, I. G.; Francey, K. F. *Eur. Polym. J.* 1979, *15*, 415-422.
38. Alam, T. M. *Radiat. Phys. Chem.* 2001, *62*, 145-152.
39. Alam, T. M.; Celina, M.; Assink, R. A.; Clough, R. L.; Gillen, K. T.; Wheeler, D. R. *Macromolecules* 2000, *33*, 1181-1190.
40. Alam, T. M.; Celina, M.; Assink, R. A.; Clough, R. L.; Gillen, K. T. *Radiat. Phys. Chem.* 2001, *60*, 121-127.
41. Labouriau, A.; Taylor, D.; Stephens, T.; Pasternak, M. *Polym. Degrad. Stab.* 2006, *91*, 1896-1902.
42. Labouriau, A.; Cox, J. D.; Schoonover, J. R.; Patterson, B. M.; Havrilla, G. J.; Stephens, T.; Taylor, D. *Polym. Degrad. Stab.* 2007, *92*, 414-424.
43. Mogon Patel, Paul Morrell, Jenny Cunningham, Robert S. Maxwell, Sarah C. Chinn, *Polym Deg. Stab*, 93 (2008) 513-519.
44. Maxwell, R. S; Cohenour, R; Sung, W; Solyom, D; Patel, M, Polym Deg Stab, 80: 443-450: (2003).
45. Patel, M; Skinner, AR; Maxwell, RS; Polym Testing, 24, 663-668, (2005).
46. Baker GK. A history of silicone stress cushions in the weapons complex. Topical

Report BDX-613-6344. Honeywell Federal Manufacturing and Technologies; June 2000. p. 1–37.
47. M.W. Blair, R.E. Muenchausen, R.D. Taylor, A. Labouriau, D.W. Cooke, T.S. Stephens; Polym Deg and Stab 93 (2008) 1585–1589
48. Andrea Labouriau, Jonathan D. Cox, Jon R. Schoonover, Brian M. Patterson, George J. Havrilla, Thomas Stephens, Dean Taylor; Polym Deg Stab 92 (2007) 414-424